Wave measurements using an ADCP? – The method and preliminary results from the East Frisian Wadden Sea, North Sea, Germany

JOERDEL, O., BARTHOLOMÄ, A. & FLEMMING, B.W.

Introduction

Today Acoustic Doppler Current Profilers (ADCP) are the standard instrumentation in the oceanographic and sedimentological survey measuring currents and suspended sediment concentration by means of acoustic backscatter. With these data processes in the water column, discharges and transport rates of suspended sediment can be calculated.

Especially in shallow water the intensity of suspended sediment transport are strongly influenced by wave activity. Mainly the wave impact controls resuspension of previously deposited fine sediments and forces the settling-lag during strong wave conditions in coastal environments. In backbarrier tidal flats of the East Frisian Islands along the North Sea coast local wave fields are mainly responsible for the resuspension of sediment. External wave fields with larger fetch lengths are only affecting the outer parts of the main tidal channels and the ebb delta between the islands.

To balance transport rates of suspended sediment inside the tidal flats investigations should be also focused to the measurements of wave parameters. Since a few years ADCP's are available which can combine measurements of current, backscatter and waves in one single system. Demonstrating the method of wave measurements by an ADCP and the presentation of preliminary results of a case study behind Spiekeroog Island are the main target of this abstract.

Study area and instrumentation

The study area is situated in the backbarrier tidal flats of the East Frisian island Spiekeroog at the German North Sea coast (Fig 1.).

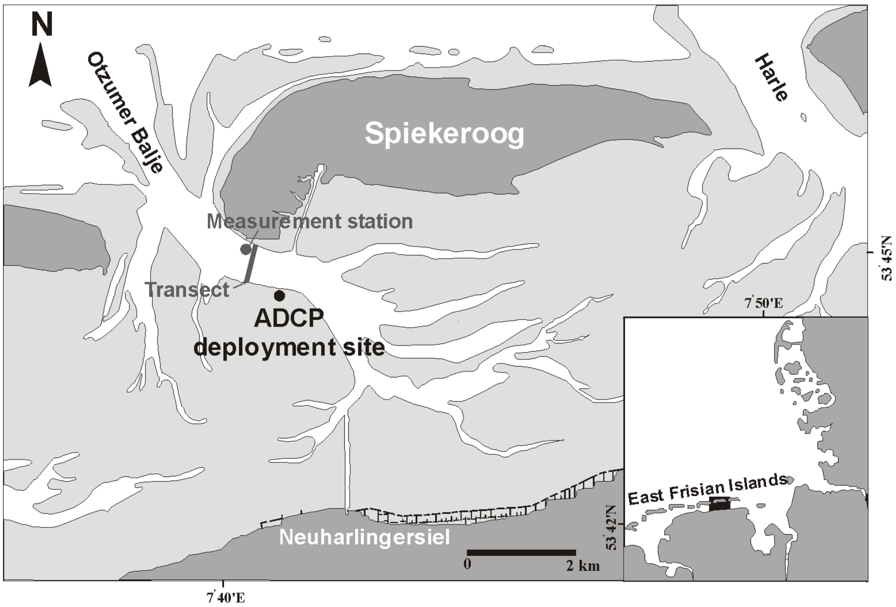

Fig. 1: Study area Spiekeroog Island and position of ADCP deployment.

Measurements for suspended sediment transport rates were carried out on a transect in the main drainage channel of the tidal inlet west of the island. Current velocities and -directions were measured by a downward-looking broadband ADCP mounted at a small research vessel running cross tracks in the channel gap.

Wave measurements have been taken by means of a 1.2 Mhz up-looking Workhorse-ADCP of RD-Instruments ™ (Fig. 2) at a locality close to the main channel on the tidal flat (Fig. 1).

These measurements were the first step preparing this system as a permanent wave record unit, which will be installed at the base of a measuring pole. There the unit should run under all weather and wave conditions.
The presented wave data records reflects the wave and current situation on an exposed tidal flat close to the main channel.

Fig. 2: Workhorse-ADCP of RD-Instruments ™.

Estimation of wave field using an ADCP

Waves are orbital motions of water. These orbital motions contain all parameters needed to characterize the wave field. These parameters in relation to the orbital motion are wave period as angular frequency, wave height as diameter of orbital corrected for the energy attenuation by depth and direction of wave propagation as orientation of the orbital in space (Fig. 3). The method to calculate waves by an ADCP is in simplification solving the measured water velocities within all bins and beams for the current and wave component.

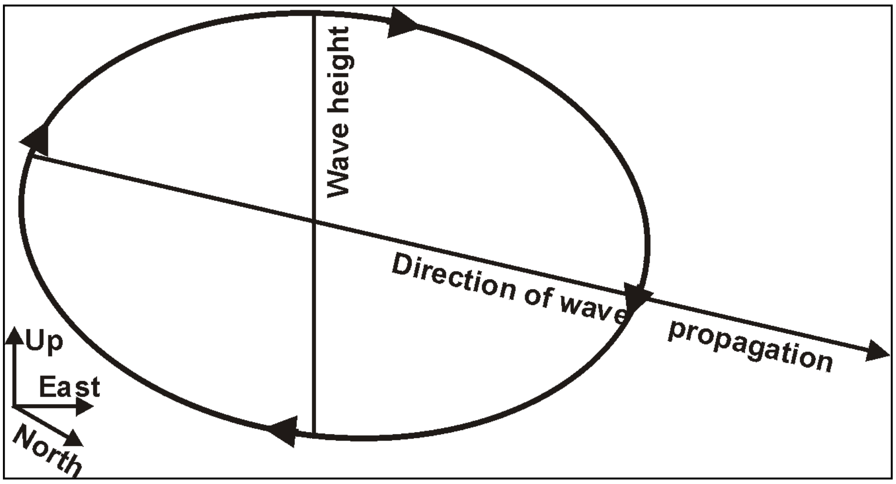

Fig. 3: Idealized wave orbital showing parameters for characterization of the wave field.

The requirements for this calculation are a stationary and homogenous wave field and an upward-looking ADCP mounting. Because of attenuation of wave energy with depth only bins near to the water surface can be used for this calculation. These bins build up an array of sensors. The aperture of this array grows with increasing distance to the transducer face. The algorithm IMLM (Iterative Maximum Likelihood Method) calculates auto- and cross-spectra bin to bin and beam to beam to estimate phase differences of orbital velocities. These phase differences are converted into horizontal and vertical velocities. These estimates are used to characterise the wave field by the parameters wave period, height and wave direction.

A less computing intense processing step can be used if no directional information of the wave field is needed. Wave height and period are calculated in this case either by using the instruments internal pressure sensor or the acoustically derived water surface range.

Results and Discussion

During the measurements over the 6th of August the wind direction was mostly southeast orientated and the water depth reached 2.6 m at high water. Visual observations showed a significant wave height of 0.1 metres and a wave period of approximately two seconds. The wave field in the tidal flats is only steady for short time periods and varies with the water depth.

For calculating the wave field we had to measure the water velocities over 20 minutes minimum in the burst mode. To measure this data in extremely shallow water areas only acoustic cells (bins) near to the transducer head can be used for the calculation, because the small water depth made it impossible to eliminate side-lobe influences.

We found a minimum valid water depth of 1.5 m for calculating the velocity derived spectra. For our case a time period of 4.5 hours was given to measure directional wave spectra over slack water.

The calculated wave frequency spectra derived from the computation by means of pressure, surface range and velocity show a good peak fit of wave height and frequency for velocity and surface range (Fig. 4). Pressure values are continuously lower and increase in wave height with frequency (Fig. 4). It can also be shown that the wave spectra are build up by a superposition of many frequencies.

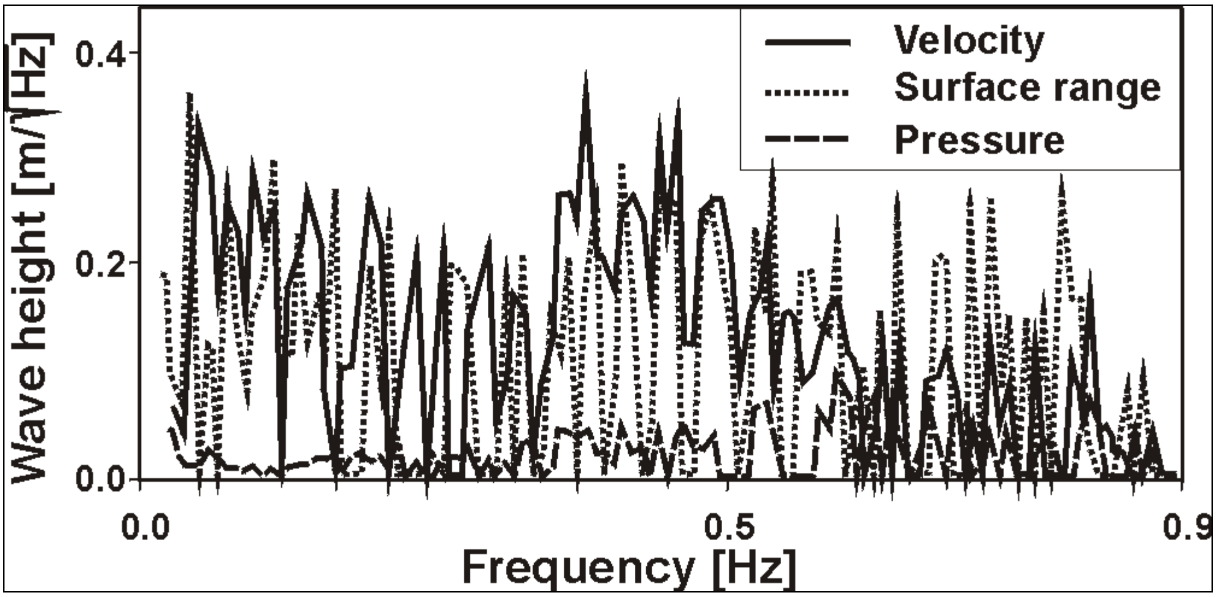

Fig. 4: Plot of wave spectra derived by pressure, surface range and orbital velocity.

Main problem in processing was the determination of upper and lower frequency thresholds to have an appropriate frequency window to match the local wave conditions. Without manual given frequency thresholds the processing software estimated wave periods of 20 up to 30 seconds, which would be 5 times larger than the mean value for open southern North Sea. We believe that this occurs through strong interferences with side lobes and multiple reflections at the surface and bottom because of the extreme shallow water conditions on the tidal flats.

Also estimates of the direction of wave propagation showed the superpostion of different waves. Plots of directional wave spectra (Fig. 5) showed waves arriving from different directions. In most cases it was not possible to clearly identify a main wave direction. The here illustrated plot shows a peak in wave energy arriving from the west. But visual observations showed mean wave direction coming from the opposite direction. As these estimates vary considerably with time (Fig. 5) we interpret this effect by the difficult environmental conditions for wave measurements. So we had to deploy the ADCP very close to the edge of the tidal flat trying to achieve a larger water depth during high water. But this position was so close to the edge, that we assume effects like refraction due to decreasing water depth had an influence on our measurements violating the requirements of an homogenous and stationary wave field.

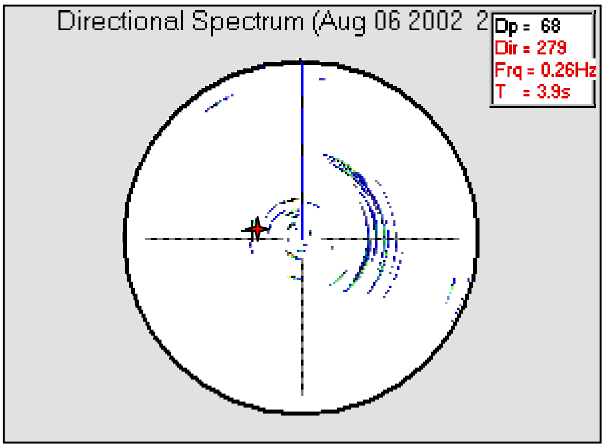

Fig. 5: Plot of directional spectrum of wave field above tidal flat. Wave frequencies plotted in this polar diagram are increasing from 0 Hz at the center to 0.9 Hz at the outer margin. Peak waves (cross) occured at at period of 3.9 sec and propagated from the west.

The evolution of the local wave field above a tidal flat is stricly correlated to the varying water depth and tidal currents (Fig. 6 a and Fig. 6b). The latter are directed during flood to the east and change their direction to the west at high water slack. During the ebb phase the current direction shifts southward reflecting the presence of a small tidal creek about 25 m south of the instrument location. Current velocities are higher during flood (up to 0.6 m/sec) than during the ebb phase. The velocity decreases to a minimum value of 0.15 m/sec around high water slack. Surprisingly the ebb current starts right after slack water at his maximum speed of 0.3m/sec and decreases nearly linear afterwards. This might be due to the drainage by the small creek south of the deployment site. The wave period shows a significant increase in peak wave period after slack water (Fig. 6c). Also mean wave period decreases slightly after high water. In contrast is the development of the significant wave height (Fig. 6d). Maximum values of 0.15 m occur before high water. During ebb current the wave height remains under 0.1 m. The diagram of direction of propagation of the wave peak displays clearly the biassed directional information (Fig. 6e).

The trend in wave periods and significant wave height may be explained in relation to the tidal current and the wind forcing. The wave field is higher and shorter in period during the flood current than during the ebb phase. During flood phase the opposing tidal and air currents create a steep wave field. The maximum wave height coincides with the maximum water current velocity. After turning of the tidal current both forcings are in the same direction resulting in a smooth wave field.

Solving the directional wave spectra seems to be impossible for this instrument position. The directions are shifting too often and in a too extreme way (Fig. 6e). We suppose that this is due to the instable wave field at the edge of the tidal flat incorporating processes such as wave refraction and reflection into our measurements and operating the ADCP close to its technical limitation. We tried to solve these problems by deploying the ADCP also far in the middle of another tidal flat, but data recording failed during that deployment.

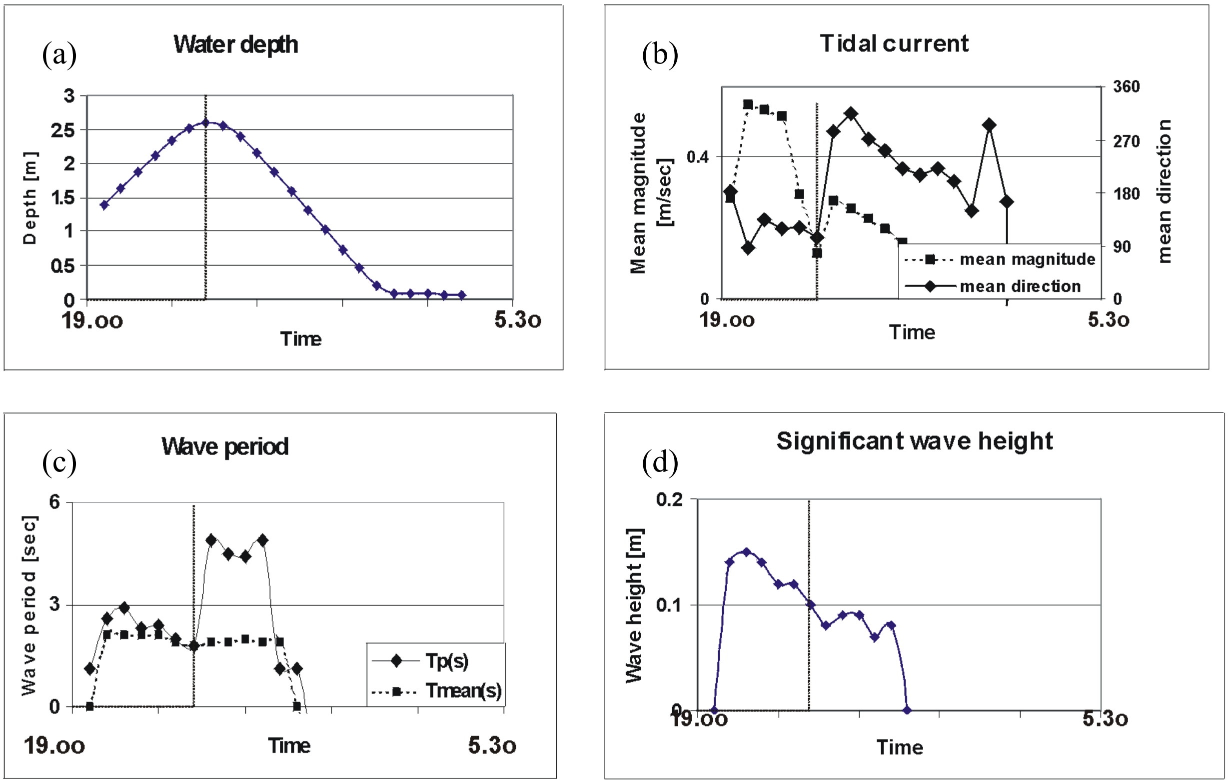

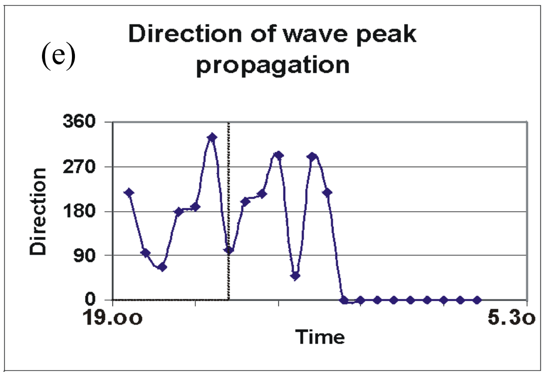

Fig. 6: Wave field parameters over one tidal half cycle (the vertical line marks high water).

Regarding the suspended sediment concentration we still have to deal with the backscatter intensity (Fig. 7). The plot confuses with the multiple reflections at the water surface due to missing surface tracking capabilities of the ADCP during wave measurements. These multiple water surface reflectors may illustrate the difficulties in directional spectra computation due to the small water depth. The contourplot illustrates clearly the higher suspended sediment load during flood due to wave-induced resuspension and the minimum in load around high water slack.

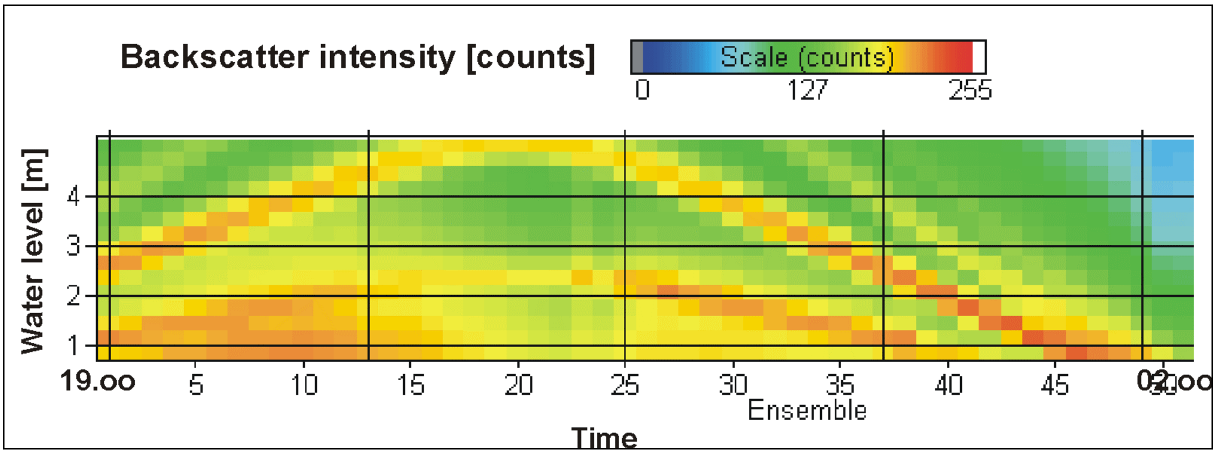

Fig. 7: Acoustic backscatter intensity over tidal half cycle.

Conclusions and further outlook

The RD-Instruments ™ high-frequency ADCP has been deployed in extreme environmental conditions such as very small water depth and instationary wave field. But careful analysis of the recorded data provide valuable information on the evolution of the wave field above tidal flats. Processing has to be handled with care as small variations of frequency thresholds lead to significant changes in processing results. For regular surveys of wave fields on tidal flats or other areas with extremely small water depth we would suggest to construct specialised ADCPs with increased beam angle for suppressing the multiple reflections.

With the deployment of the ADCP at the soon ready equipped measuring pole we will deploy our ADCP in a much more suitable environment. Hydrodynamic parameters like current velocities and –direction and the local wave field will be surveyed continously during all weather conditions. In-situ settling velocitiy and aggregate size measurements by laser diffraction will be included into the schedule.

We expect these surveys to provide more detailed data for analysing relations between hydrodynamic conditions and the transport of suspended sediment within the tidal basin.